

## EFFECT OF THERMAL RADIATION ON FREE CONVECTION FLOW AND HEAT TRANSFER OVER A TRUNCATED CONE IN PRESENCE OF PRESSURE WORK AND HEAT GENERATION/ABSORPTION

by

**Elsayed M. A. ELBASHBESHY<sup>a</sup>, Tarek G. EMAM<sup>b</sup>, and Emad A. SAYED<sup>c</sup>**

<sup>a</sup> Mathematics Department, Faculty of Science, Ain Shams University, Abbassia, Cairo, Egypt

<sup>b</sup> Department of Mathematics, Jeddah University in Khulais, Saudi Arabia

<sup>c</sup> Department of Physics & Engineering Mathematics, Faculty of Engineering-Mattaria  
Helwan University, Cairo, Egypt

Original scientific paper  
DOI: 10.2298/TSCI130409006E

*Effect of heat generation or absorption and thermal radiation on free convection flow and heat transfer over a truncated cone in the presence of pressure work is considered. The governing boundary layer equations are reduced to non-similarity boundary layer equations and solved numerically by using Mathematica technique. Comparisons with previously published work on special cases of the problem are performed and the results are found to be in excellent agreement. The solutions are presented in terms of local skin friction, local Nusselt number, velocity, and temperature profiles for values of Prandtl number, pressure work parameter, radiation parameter, and heat generation or absorption parameter.*

Key words: *laminar boundary layer, pressure work, vertical truncated cone, heat transfer, thermal radiation, heat generation/absorption*

### Introduction

Free convection flow is often encountered in cooling of nuclear reactors or in the study of the structure of stars and planets. The study of temperature and heat transfer is of great importance to the engineers because of its almost universal occurrence in many branches of science and engineering. The discussion and analysis of free convection flows and pressure work effects are generally ignored but here we have considered the effect of pressure work on a free convection flow along a vertical truncated cone.

Numerous authors have investigated laminar free convection flows, especially in the case of non-uniform surface temperature. Mark and Prins [1, 2] developed the general relations for similar solutions on isothermal axisymmetric forms and showed that for the flow past a vertical cone has such a solution. The free convection similarity flows about 2-D axisymmetric bodies with closed lower ends has been studied by Braun *et al.* [3]. Similarity solutions for free convection from the vertical cone have been exhausted by Hering and Grosh [4]. Hering and Grosh [4] have been extended by Roy [5] for the case of high values of the Prandtl number. Na and Chiou [6] presented the laminar natural convection over a frustum of a cone without a transverse curvature effect. Alamgir [7] used an integral method to study the overall heat transfer from vertical cones in laminar natural convection. The effect of viscous

\* Corresponding author; e-mail: elbashbeshy100@hotmail.com

dissipation and pressure stress work in natural convection along a vertical isothermal plate has been studied by Pantokratoras [8]. The laminar free convection flow from a vertical circular cone maintained at non-uniform surface temperature with suction and pressure work has been studied by Alim *et al.* [9]. Alam *et al.* [10] investigated the laminar free convection flow from a vertical permeable circular cone maintained at non-uniform surface temperature with pressure work. Hossain and Paul [11] investigated the laminar free convection from a vertical permeable circular cone with non-uniform surface without pressure work. Elbashbeshy *et al.* [12] investigated the laminar free convection from a vertical circular cone with variable surface heat flux in the presence of the pressure work.

In this analysis we consider the volumetric rate of heat generation:

$$q''' = \begin{cases} Q_0(T - T_\infty) & \text{for } T \geq T_\infty \\ 0 & \text{for } T \leq T_\infty \end{cases}$$

The effect of heat generation/absorption on free convective has been studied by scientists and technologists [13-17]. The effects of heat generation/absorption and thermal radiation on mixed convection flow over an unsteady stretching permeable surface has been studied by Shakhaooth Khan *et al.* [18, 19].

As the difference between the surface temperature and the ambient temperature is large. The radiation effect becomes important. In the aspect of convection radiation, Viskanta and Grosh [20] considered the effect of thermal radiation on the temperature distribution and the heat transfer in an absorbing and emitting media flowing over a wedge by using the Rosseland diffusion approximation. This approximation leads to a considerable simplification in the expression for the radiant flux. Later, a natural convection radiation interaction in the boundary-layer flow over horizontal surface was presented by Chen *et al.* [21]. In [20, 21], the temperature difference within the flow are assumed to be sufficiently small such that  $T^4$  may be expressed as a linear function of temperature, *i.e.*  $T^4 \approx 4T_\infty^3T - 3T_\infty^4$ . Hossain and Alim [22] and Hossain and Rees [23] investigated the natural convection-radiation interaction on a boundary-layer flow along thin vertical cylinder [22], an isothermal plate inclined at a small angle to the horizontal [23].

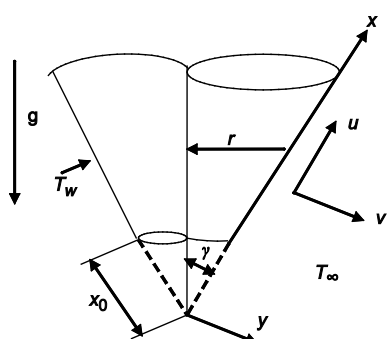


**Figure 1. Physical model and co-ordinates system**

The purpose of this paper, therefore, is extended the study of Elbashbeshy *et al.* [12] to consider the effect of thermal radiation on the free convection flow and heat transfer over a truncated cone in the presence of pressure work and internal heat generation/absorption.

### Mathematical formulation

We consider the steady-state 2-D, laminar free convection boundary layer flow near a vertical truncated cone as shown in fig. 1. The origin of the co-ordinates system is placed at the vertex of the cone, where  $x$  co-ordinate along the surface of the cone is measured from the origin and  $y$  co-ordinate is normal to the surface of the cone. The distance of the leading edge of the truncated cone measured from the origin is denoted as  $x_0$ . The surface of the truncated cone is held at a constant temperature  $T_w$  which is higher than the ambient fluid temperature  $T_\infty$ . The fluid properties are assumed to be constant except for density variations in buoyancy force term.

measured from the origin is denoted as  $x_0$ . The surface of the truncated cone is held at a constant temperature  $T_w$  which is higher than the ambient fluid temperature  $T_\infty$ . The fluid properties are assumed to be constant except for density variations in buoyancy force term.

The boundary layer equations for steady laminar boundary layer along a vertical cone as [9, 12] are given:

$$u \frac{\partial u}{\partial x} + v \frac{\partial u}{\partial y} = 0 \quad (1)$$

$$u \frac{\partial u}{\partial x} + v \frac{\partial u}{\partial y} = v \frac{\partial^2 u}{\partial y^2} + g \beta \cos \gamma (T - T_\infty) \quad (2)$$

$$u \frac{\partial T}{\partial x} + v \frac{\partial T}{\partial y} = \alpha \frac{\partial^2 T}{\partial y^2} + \frac{T \beta u}{\rho C_p} \frac{\partial p}{\partial x} + \frac{\alpha Q_0}{k} (T - T_\infty) - \frac{1}{\rho C_p} \frac{\partial q_r}{\partial y} \quad (3)$$

The boundary conditions are given by:

$$\begin{aligned} u &= 0, & v &= 0, & T &= T_w & \text{at} & & y = 0 \\ u &= 0, & T &= T_\infty & \text{as} & & y \rightarrow \infty \end{aligned} \quad (4)$$

For exterior conditions, we known hydrostatic pressure is  $\partial p / \partial x = \rho g$ .

Using the Rosseland approximation for radiation [24], radiative heat flux is simplified:

$$q_r = - \frac{4 \sigma}{3 \alpha^*} \frac{\partial T^4}{\partial y} \quad (5)$$

Assuming that the temperature differences within the flow is such that the term  $T^4$  may be expressed as a linear function of temperature. Hence, expanding  $T^4$  in a Taylor series about  $T_\infty$  and neglecting higher-order terms we get:

$$T^4 \cong 4T_\infty^3 T - 3T_\infty^4 \quad (6)$$

Using eqs. (5) and (6), the energy eq. (3) becomes:

$$u \frac{\partial T}{\partial x} + v \frac{\partial T}{\partial y} = \alpha \frac{\partial^2 T}{\partial y^2} + \frac{T \beta u}{\rho C_p} \frac{\partial p}{\partial x} + \frac{16 \sigma T_\infty^3}{3 \alpha^* \rho C_p} \frac{\partial^2 T}{\partial y^2} + \frac{Q_0}{\rho C_p} (T - T_\infty) \quad (7)$$

The continuity equation can be satisfied by introducing the stream function  $\psi$  such that:

$$u = \frac{1}{r} \frac{\partial \psi}{\partial y} \quad \text{and} \quad v = - \frac{1}{r} \frac{\partial \psi}{\partial x} \quad (8)$$

Applying the following transformations:

$$\begin{aligned} \xi &= \frac{x^*}{x_0} = \frac{x - x_0}{x_0}, & \eta &= \frac{y}{x^*} (\text{Gr}_{x^*})^{1/4}, & \text{Gr}_{x^*} &= \frac{g \beta \cos \gamma (T_w - T_\infty) x^{*3}}{v^2}, \\ \psi &= v r (\text{Gr}_{x^*})^{1/4} f(\xi, \eta), & T - T_\infty &= (T_w - T_\infty) \theta(\xi, \eta), \end{aligned}$$

$$\begin{aligned} u &= \frac{\nu(\text{Gr}_{x^*})^{1/2}}{x^*} f' = U_r f' \\ v &= -\frac{\nu(\text{Gr}_{x^*})^{1/4}}{x^*} \left[ \left( \frac{\xi}{\xi+1} + \frac{3}{4} \right) f' + \xi \frac{\partial f}{\partial \xi} - \frac{1}{4} \eta f' \right] \end{aligned} \quad (9)$$

Substituting the transformations given in (6) into eqs. (1)-(4), we obtain:

$$f''' + \left( \frac{\xi}{\xi+1} + \frac{3}{4} \right) ff'' - \frac{1}{2} f'^2 + \theta = \xi \left( f' \frac{\partial f'}{\partial \xi} - f'' \frac{\partial f}{\partial \xi} \right) \quad (10)$$

$$\left( \frac{1}{\text{Pr}} + \frac{N_R}{\text{Pr}} \right) \theta'' + \left( \frac{\xi}{\xi+1} + \frac{3}{4} \right) f \theta' - \epsilon f' \theta + \delta \theta = \xi \left( f' \frac{\partial \theta}{\partial \xi} - \theta' \frac{\partial f}{\partial \xi} \right) \quad (11)$$

The corresponding boundary conditions to be satisfied are:

$$\begin{aligned} f &= f' = 0, & \theta &= 1 & \text{at } \eta = 0 \\ f' &= 0, & \theta &= 0 & \text{as } \eta \rightarrow \infty \end{aligned} \quad (12)$$

where the primes denote the differentiation with respect to  $\eta$ . The  $x^*$  is the distance measured from the leading edge of the truncated cone. The  $\text{Gr}_{x^*}$  is the local Grashof number based upon  $x^*$ ,  $\text{Pr} = \nu/\alpha$  – the Prandtl number,  $N_R = 16\sigma T_\infty^3/3k\alpha$  – the radiation parameter,  $\delta = (\alpha Q_0/\nu k)(x^*)^3(\text{Gr}_{x^*})^{-1/2}$  – the heat generation/absorption parameter, and  $\epsilon = g\beta x^*/C_p$  – the pressure work parameter which is first used by Gebhart [25]. Equations (10) and (11) subjected to the boundary conditions (12) are solved by using Mathematica program. The quantities of physical interest are the local skin friction coefficient  $C_f$  and the local Nusselt number  $\text{Nu}_{x^*}$  are defined:

$$C_f = \frac{2\tau_w}{\rho U_r^2} \quad \text{and} \quad \text{Nu}_{x^*} = -\frac{q_w x^*}{k(T_w - T_\infty)}$$

$$\text{where } \tau_w = \mu \left( \frac{\partial u}{\partial y} \right)_{y=0} \quad \text{and} \quad q_w = -k \left( \frac{\partial T}{\partial y} \right)_{y=0} + (q_r)_{y=0}$$

are the shear stress and rate of heat-flux at the surface, respectively, and  $U_r = \nu(\text{Gr}_{x^*})^{1/2}/x^*$  is the reference velocity.

Using the transformation (6), then  $C_f$  and  $\text{Nu}_{x^*}$  take the form:

$$\begin{aligned} \frac{1}{2} (\text{Gr}_{x^*})^{1/4} C_f &= f''(\xi, 0) \\ \frac{\text{Nu}_{x^*}}{(\text{Gr}_{x^*})^{1/4}} &= (1 + N_R) [-\theta'(\xi, 0)] \end{aligned}$$

### Numerical solution

Equations (10) and (11) subject to the boundary condition (12) are converted into the following simultaneous system of first order:

$$\begin{aligned}
 y'_1 &= y_2, & y'_2 &= y_3 \\
 y'_3 &= \frac{1}{2} y_2^2 - \left( \frac{\xi}{\xi+1} + \frac{3}{4} \right) y_1 y_3 - y_4 \\
 y'_4 &= y_5 \\
 y'_5 &= \frac{\Pr}{1+N_R} \left[ \epsilon y_2 y_4 - \delta y_4 - \left( \frac{\xi}{\xi+1} + \frac{3}{4} \right) y_1 y_5 \right]
 \end{aligned} \tag{13}$$

where  $y_1 = f$  and  $y_4 = \theta$ .

Subjected to the initial conditions:

$$y_1(0) = 0, \quad y_2(0) = 0, \quad y_3(0) = s_1(\xi), \quad y_4(0) = 1, \quad y_5(0) = s_2(\xi) \tag{14}$$

where  $s_1$  and  $s_2$  are unknown to be determined as a part of the numerical solution.

Using Mathematica, a function  $F(s_1, s_2)$  has been defined such that  $F[s_1, s_2] = \text{NDSolve}[system \ (13, 14)]$ . The values of  $s_1$  and  $s_2$  are determined upon solving the equations  $y_2(\eta_{\max}) = 0$ , and  $y_4(\eta_{\max}) = 0$  to get the solution, NDSolve first searches for initial conditions that satisfy the equations, using a combination of Solve and a procedure much like Find Root. Once  $s_1$  and  $s_2$  are determined, the system (13) and (14) is closed, it can be solved numerically using the NDSolve function.

## Results and discussion

The set of non-linear partial differential eqs. (10) and (11) satisfying the boundary conditions (12) have been solved numerically using the MATHEMATICA method for several values of the involved parameters, namely Prandtl number, radiation parameter,  $N_R$ , heat generation/absorption parameter,  $\delta$ , and pressure work parameter,  $\epsilon$ . For validation of numerical method used in this study the case when  $\epsilon = 0$  (the pressure work parameter is absent),  $\delta = 0$  (no heat source/sink), and  $N_R = 0$  (no radiation) has also been considered and the results are compared with those of Cebeci and Bradshaw [26], Na [27], Na and Chiou [6], Kays and Crawford [28], Lin and Chen [29], Hering and Grosh [4], Roy [5], and Alamgir [7]. The quantitative comparison is shown in tabs. 1 and 2 and it is found to be in a very excellent agreement. Here  $\infty$  denotes  $\xi = 10^4$ .

**Table 1. Comparison of values of  $f''(0, 0)$  and  $-\theta(0, 0)$  for various values of  $\Pr$  (0.1, 1, 10) with  $\epsilon = \delta = N_R = 0$**

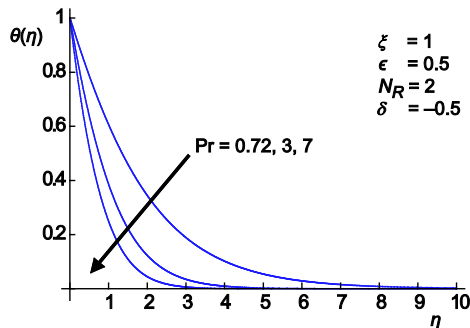
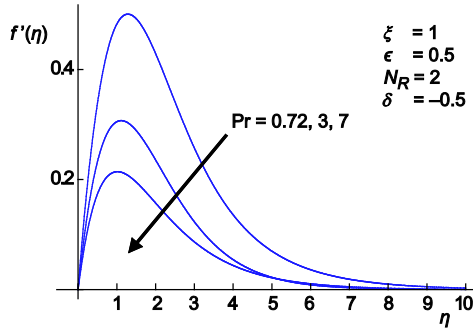
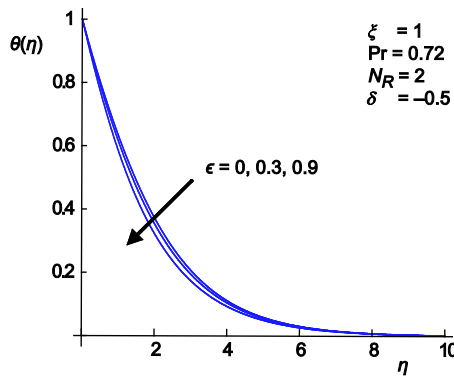
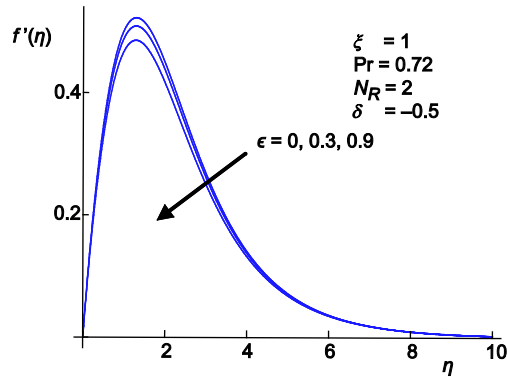
$f''(0, 0)$			$-\theta(0, 0)$					
$\Pr$	Ref. [26]	Present results	Ref. [27]	Ref. [6]	Ref. [3]	Ref. [28]	Ref. [29]	Present results
0.1	1.2104	1.2151	—	—	0.1637	0.164	0.1627	0.1627
1	0.9081	0.9082	0.4010	0.4011	0.4009	0.4010	0.4009	0.4010
10	0.5930	0.5928	0.8269	0.8269	0.8266	0.8270	0.8258	0.8268

The effects of Prandtl number, pressure work parameter  $\epsilon$ , radiation parameter  $N_R$ , heat generation/absorption parameter  $\delta$ , and the dimensionless distance,  $\xi$ , on the dimensionless velocity profiles,  $f(\eta)$ , and temperature profiles,  $\theta(\eta)$ , are shown in figs. 2-11.

**Table 2. Comparison of values of  $f''(\infty, 0)$  and  $-\theta(\infty, 0)$  for various values of Pr (0.1, 1, 10) with  $\epsilon = \delta = N_R = 0$** 

f''( $\infty, 0$ )				-θ( $\infty, 0$ )				
Pr	Ref. [4]	Ref. [5]	Present results	Ref. [4]	Ref. [5]	Ref. [7]	Ref. [6]	Present results
0.1	1.0960	—	1.0959	0.2113	—	0.2141	—	0.2113
1	0.7694	0.8600	0.7694	0.5104	0.5275	0.5280	0.5104	0.5104
10	—	0.4899	0.4877	—	1.0354	1.0159	1.0340	1.0340

Figures 2 and 3 show the effects of vary Prandtl number on the dimensionless velocity and dimensionless temperature against  $\eta$  for the pressure work parameter,  $\epsilon = 0.5$ , radiation parameter,  $N_R = 2$ , heat generation/absorption parameter,  $\delta = -0.5$ , and the dimensionless distance,  $\xi = 1$ . It is observed that the velocity and temperature profiles are decreases with increasing value of Prandtl number. In the case of water at 20 °C ( $\text{Pr} = 7.0$ ), the free laminar boundary show a sharp decrease compared to effects in air at 20 °C ( $\text{Pr} = 0.72$ ). Figures 4 and 5 shows the velocity and temperature profiles for pressure work parameter  $\epsilon$  with radiation parameter,  $N_R = 2$ , heat generation/absorption parameter,  $\delta = -0.5$ , the dimensionless distance,

**Figure 2. The temperature profiles  $\theta(\eta)$  for various Prandtl numbers****Figure 3. The velocity profiles  $f'(\eta)$  for various Prandtl numbers****Figure 4. The temperature profiles  $\theta(\eta)$  for various  $\epsilon$** **Figure 5. The velocity profiles  $f'(\eta)$  for various  $\epsilon$**

$\zeta = 1$ , and  $\text{Pr} = 0.72$ . From these figures it is seen that, the velocity and temperature profiles are decreases with the increasing value of  $\epsilon$ . From figs. 6 and 7 we observe that, the velocity and temperature profiles increases with increasing of radiation parameter  $N_R$  with other parameters  $\text{Pr} = 0.72$ ,  $\epsilon = 0.5$ ,  $\delta = -0.5$ , and  $\zeta = 1$ . In figs., 8 and 9 the effects of heat generation/absorption parameter  $\delta$  on the dimensionless velocity and dimensionless temperature for the pressure work parameter  $\epsilon = 0.5$ , radiation parameter  $N_R = 2$ ,  $\text{Pr} = 0.72$ , and the dimensionless distance  $\zeta = 1$ . It is observed that the velocity and temperature profiles are increases with increasing value of  $\delta$ . From figs. 10 and 11 we observe that, the velocity and temperature

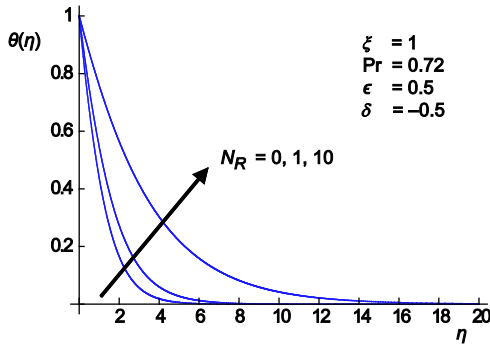


Figure 6. The temperature profiles  $\theta(\eta)$  for various  $N_R$

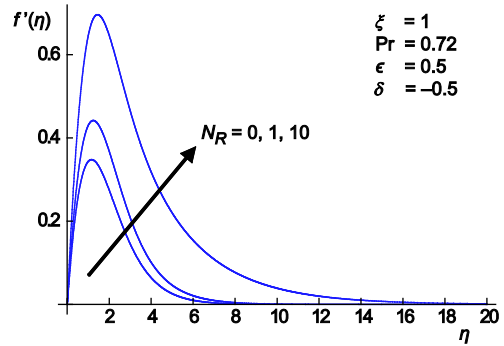


Figure 7. The velocity profiles  $f'(\eta)$  for various  $N_R$

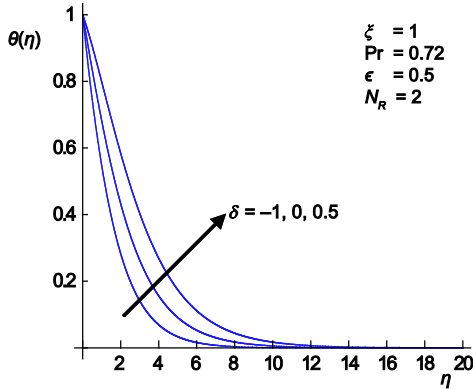


Figure 8. The temperature profiles  $\theta(\eta)$  for various  $\delta$

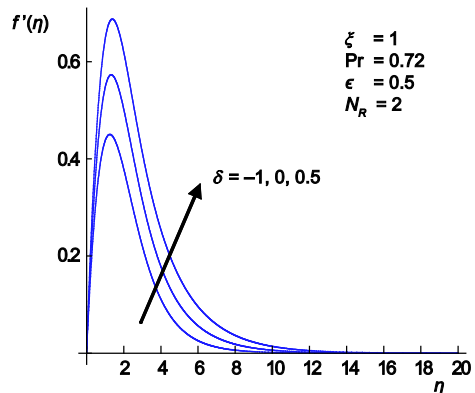


Figure 9. The velocity profiles  $f'(\eta)$  for various  $\delta$

profiles decreases with the increasing of the dimensionless distance  $\zeta$  with other parameters  $\text{Pr} = 0.72$ ,  $\epsilon = 0.5$ ,  $N_R = 2$ , and  $\delta = -0.5$ . In figs., 12 and 13 the effects of radiation parameter  $N_R$  on the local skin friction coefficient and local Nusselt number are observed. From these figures, it can be seen that an increase in the value of  $N_R$  leads to an increase in the values of the local skin friction coefficient. Also, we observe that the local Nusselt number decrease with the increase of the radiation parameter. When  $\zeta$  is very small and large the local skin friction coefficient and the local Nusselt number become constant. In figs. 14 and 15, the effects of Prandtl number on the local skin friction coefficient and local Nusselt number are observed. From these figures, it can be seen that an increase in the value of Prandtl number leads to a decrease in the values of the local skin friction coefficient. Also, we observe that the local

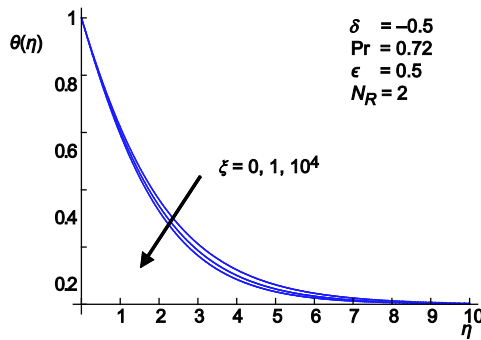


Figure 10. The temperature profiles  $\theta(\eta)$  for various  $\xi$

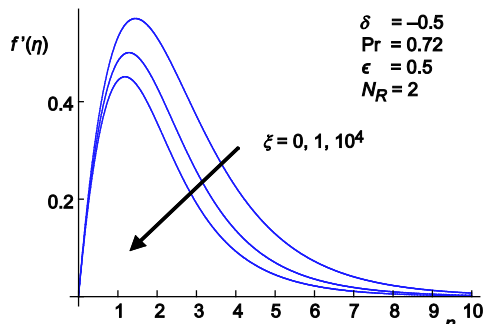


Figure 11. The velocity profiles  $f'(\eta)$  for various  $\xi$

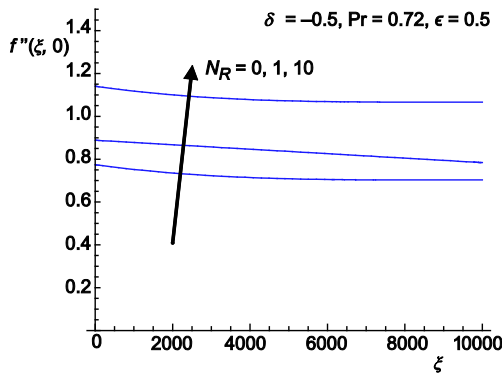


Figure 12. The skin-friction coefficient for various  $N_R$

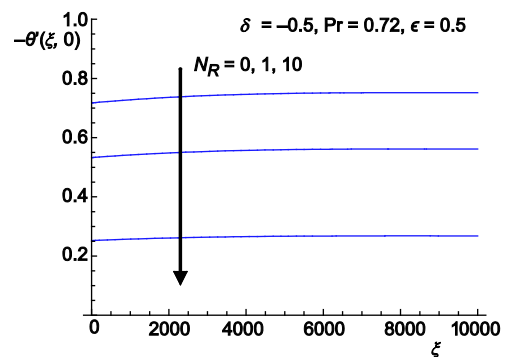


Figure 13. The Nusselt number for various  $N_R$

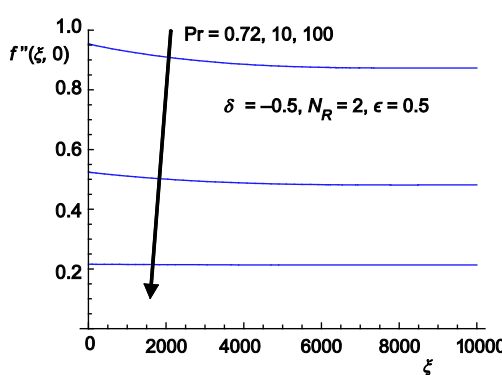


Figure 14. The skin-friction coefficient for various Prandtl numbers

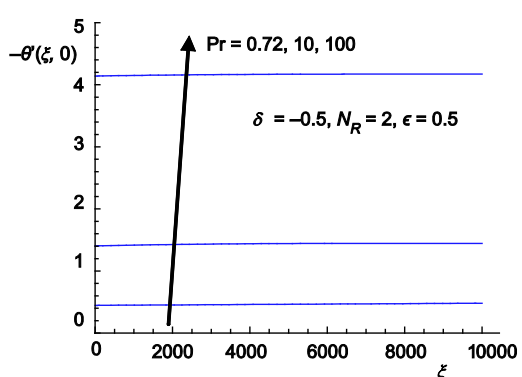


Figure 15. The Nusselt number for various Prandtl numbers

Nusselt number increase with the increase of the Prandtl number parameter. In figs. 16 and 17, the effect of heat generation/absorption parameter,  $\delta$ , on the local skin friction coefficient and local Nusselt number are observed. From these figures, it can be seen that an increase in the value of generation/absorption parameter  $\delta$  leads to an increase in the values of skin friction coefficient and decrease in the value of local Nusselt number. In figs. 18 and 19, the effects of pressure work parameter,  $\epsilon$ , on the local skin friction coefficient and local Nusselt number are

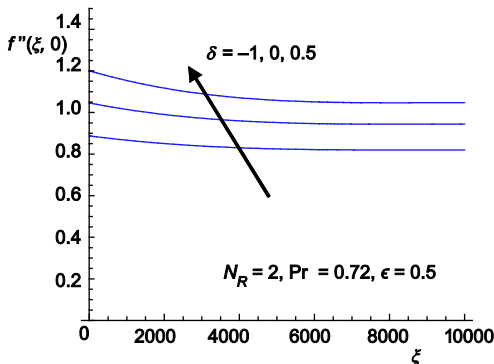


Figure 16. The skin-friction coefficient for various  $\delta$

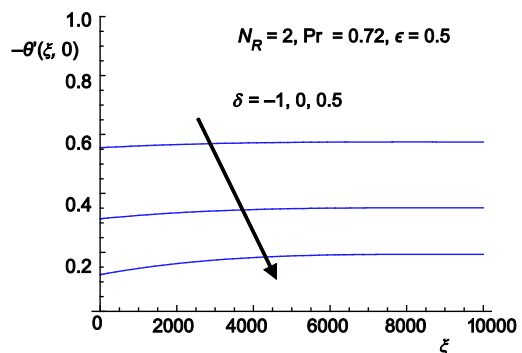


Figure 17. The Nusselt number for various  $\delta$

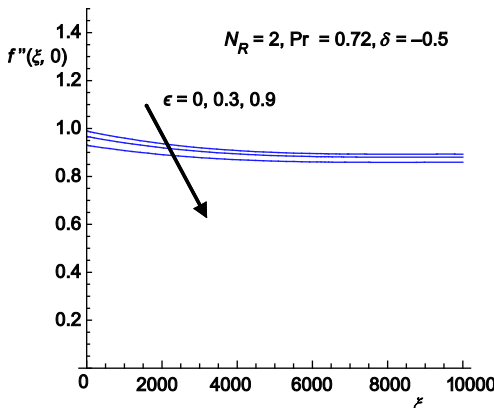


Figure 18. The skin-friction coefficient for various  $\epsilon$

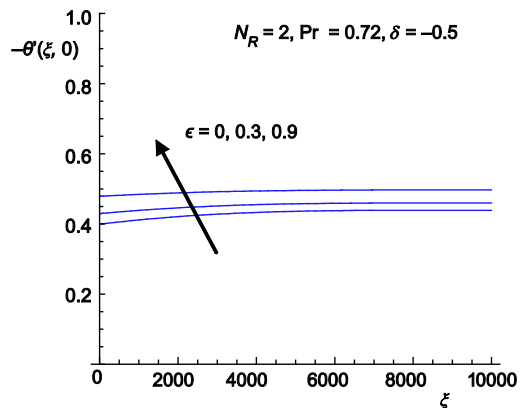


Figure 19. The Nusselt number for various  $\epsilon$

observed. From these figures, it can be seen that an increase in the value of pressure work parameter leads to a decrease in the values of skin friction coefficient and increase in the value of local Nusselt number. When  $\xi$  is very small and large the local skin friction coefficient and the local Nusselt number becomes constant.

### Conclusions

In this paper, the problem of steady, laminar free convection from a truncated vertical cone with pressure work in the presence of radiation parameter and heat generation/absorption parameter is studied. From the present investigations, we may conclude as following.

- It is cleared that the velocity and temperature distribution decreases with increasing the values of  $\epsilon$ ,  $Pr$ , and  $\xi$  while the velocity and temperature distribution increases with increasing the values of  $N_R$ , and  $\delta$ .
- For increasing values of the pressure work parameter  $\epsilon$  and Prandtl number, the skin friction coefficient decreases but local Nusselt number increase.
- An increasing in the values of radiation parameter,  $N_R$ , and heat generation/absorption parameter  $\delta$  leads to increases in the value of the skin friction coefficient while the local Nusselt number decreases.

## Nomenclature

$C_p$	– specific heat at constant pressure, [ $\text{Wm}^{-1}\text{K}^{-1}$ ]	$y$	– co-ordinate normal to the surface of the truncated cone, [m]
$C_f$	– local skin friction coefficient, [-]		
$f$	– dimensionless stream function, [-]		
$g$	– gravitational acceleration, [ $\text{ms}^{-2}$ ]		
$\text{Gr}_{x^*}$	– the local Grashof number, [-]		
$k$	– thermal conductivity, [ $\text{Wm}^{-1}\text{K}^{-1}$ ]		
$N_R$	– radiation parameter, [-]		
$\text{Nu}_{x^*}$	– local Nusselt number, [-]		
$\text{Pr}$	– Prandtl number, [-]		
$p$	– fluid pressure, [Pa]		
$Q_0$	– heat generation/absorption, [K]		
$q_r$	– radiation heat flux, [ $\text{Km}^{-2}$ ]		
$r$	– local radius of the truncated cone, [m]		
$T$	– temperature of the fluid, [K]		
$T_\infty$	– temperature of the ambient fluid, [K]		
$u$	– fluid velocity component in the x-direction, [ $\text{ms}^{-1}$ ]		
$v$	– fluid velocity component in the y-direction, [ $\text{ms}^{-1}$ ]		
$x$	– measured from the leading edge, [m]		
$x_0$	– distance of the leading edge of truncated cone measured from the origin, [m]		
$x^*$	– distance measured from the leading edge of the truncated cone, [m]		

<i>Greek symbols</i>	
$\alpha$	– thermal diffusivity, [ $\text{m}^{-2}\text{s}^{-1}$ ]
$\alpha^*$	– mean absorption coefficient, [-]
$\beta$	– coefficient of volume expansion, [ $\text{K}^{-1}$ ]
$\delta$	– heat generation/absorption parameter, [-]
$\gamma$	– the cone apex half-angle, [-]
$\eta$	– the pseudo-similarity variable, [-]
$\mu$	– dynamic viscosity, [ $\text{kgms}^{-1}$ ]
$\sigma$	– Stefan Boltzman constant, [-]
$\nu$	– kinematic viscosity, [ $\text{m}^2\text{s}^{-1}$ ]
$\xi$	– dimensionless distance, [-]
$\theta$	– dimensionless temperature, [-]
$\rho$	– density of the fluid inside the boundary layer, [ $\text{kgm}^{-3}$ ]
$\psi$	– stream function, [-]
$\epsilon$	– pressure work parameter, [-]

## References

- [1] Merk, E. J., Prinss, J. A., Thermal Convection in Laminar Boundary I, *Appl. Sci. Res.*, 4A (1954), 3, pp. 11-24
- [2] Merk, E. J., Prinss, J. A., Thermal Convection in Laminar Boundary II, *App. Sci. Res.*, 4A (1954), 3, pp. 195-206
- [3] Braun, W. H., et al., Free Convection Similarity Flows about Two Dimensional and Axisymmetric Bodies with Closed Lower Ends, *Int. J. Heat and Mass Transfer*, 2 (1961), 1-2, pp.121-135
- [4] Hering, R. G., Grosh, R. J., Laminar Free Convection from a Non-Isothermal Cone, *Int. Heat and Mass Transfer*, 5 (1962), 11, pp. 1059-1068
- [5] Roy, S., Free Convection over a Slender Vertical Cone at High Prandtl Numbers, *ASME J. Heat Mass Transfer*, 101 (1974), Feb., pp. 174-176
- [6] Na, T. Y., Chiou, J. P., Laminar Natural Convection over a Frustum of a Cone, *Applied Scientific Research*, 35 (1979), 5, pp. 409-421
- [7] Alamgir, M., Over-All Heat Transfer from Vertical Cones in Laminar Free Convection: An Approximate Method, *Transactions of ASME Journal of Heat Transfer*, 101 (1979), 1, pp. 174-176
- [8] Pantokratoras, A., Effect of Viscous Dissipation and Pressure Stress Work in Natural Convection along a Vertical Isothermal Plate, *Int. J. Heat Mass Transfer*, 46 (2003), 25, pp. 4979-4983
- [9] Alim, M. A., et al., Pressure Work Effect on Natural Convection from a Vertical Circular Cone with Suction and Non-Uniform Surface Temperature, *J. Mech. Eng.*, 36 (2006), Dec., pp. 6-11
- [10] Alam, Md. M., et al., Free Convection from a Vertical Permeable Circular Cone with Pressure Work and Non-Uniform Surface Temperature, *Nonlinear Analysis Modeling and Control*, 12 (2007), 1, pp. 21-32
- [11] Hossain, M. A., Paul, S. C., Vertical Permeable Circular Cone with Non-Uniform Surface Heat Flux, *Heat and Mass Transfer*, 37 (2001), 2, pp. 167-173
- [12] Elbashbeshy, E. M. A., et al., Effect of Pressure Work on Free Convection Flow from a Vertical Circular Cone with Variable Surface Heat Flux, *Strojnický Casopis*, 63 (2012), 3, pp. 169-177
- [13] Chamkha, A. J., Effects of Heat Generation/Absorption and Thermophoresis on Hydromagnetic Flow with Heat and Mass Transfer over a Flat Surface, *Int. J. Numer. Methods Fluid Flow*, 10 (2000), 4, pp. 432-439
- [14] Molla, M. M., et al., Natural Convection Flow along a Vertical Wavy Surface with Uniform Surface Temperature in the Presence Heat Generation/Absorption, *Int. J. Thermal Sci.*, 43 (2004), 2, pp. 157-163

- [15] Hady, F. M., et al., MHD Free Convection Flows along a Vertical Wavy Surface with Heat Generation or Absorption Effect, *Int. commun. Heat Mass Transfer*, 33 (2006), 10, pp. 1253-1259
- [16] Molla, M. M., et al., Natural Convection Flow from an Isothermal Horizontal Circular Cylinder in the Presence of Heat Generation, *Int. J. Eng. Sci.*, 44 (2006), 13-14, pp. 949-955
- [17] Bagai, S., Effect of Variable Viscosity on Free Convection over a Non-Isothermal Heat Generation, *Acta Mech.*, 169 (2004), 1, 187-186
- [18] Shakhaooth Khan, Md., et al., Heat Generation, Thermal Radiation and Chemical Reaction Effects on MHD Mixed Convection Flow over an Unsteady Stretching Permeable Surface, *Int. Journal of Basic and Applied Science*, 1 (2012), 2, pp. 363-377
- [19] Shakhaooth Khan, Md., et al., Non-Newtonian MHD Mixed Convective Power-Law Fluid Flow over a Vertical Stretching Sheet with Thermal Radiation, Heat Generation and Chemical Reaction Effects, *Academic Research International*, 3 (2012), 3, pp. 80-92
- [20] Viskanta, R., Grosh, R. J. Boundary Layer in Thermal Radiation Absorbing and Emitting Media, *Int. J. Heat Mass Transfer*, 5 (1962), 9, pp. 7950-806
- [21] Chen, T. S., et al., Natural Convection Interaction in Boundary-Layer Flow over Horizontal Surfaces, *AIAA Journal*, 22 (1984), 12, pp. 1797-1803
- [22] Hossain, M. A., Alim, M. A., Natural Convection-Radiation Interaction on Boundary Layer Flow along a Thin Vertical Cylinder, *Heat Mass Transfer*, 32 (1997), 6, pp. 515-520
- [23] Hossain, M. A., Rees, D. A. S., Free Convection-Radiation Interaction from an Isothermal Plate Inclined at a Small Angle to the Horizontal, *Acta Mechanica*, 127 (1998), 1, pp. 63-73
- [24] Chen, C. H., MHD Mixed Convection of a Power-Law Fluid Past a Stretching Surface in the Presence of Thermal Radiation and Internal Heat Generation/Absorption, *Int. J. of Nonlinear Mechanics*, 44 (2008), 6, pp. 296-603
- [25] Gebhart, B., Effects of Viscous Dissipation in Natural Convection, *Journal of Fluid Mech.*, 14 (1962), 2, pp. 225-232
- [26] Cebeci, T., Bradshaw, P., *Physical and Computational Aspects of Convective Heat Transfer*, 1<sup>st</sup> ed., Springer, New York, USA, 1984, pp. 270-275
- [27] Na, T. Y., Numerical Solution of Natural Convection Flow Past a Non-Isothermal Vertical Flat Plat, *Applied Scientific Research*, 33 (1977), 5, pp. 519-543
- [28] Kays, W. M., Crawford, M. E., *Convective Heat and Mass Transfer*, 3<sup>rd</sup> ed., McGraw-Hill, New York, USA, 1980, pp. 402-410
- [29] Lin, H. T., Chen, C. C., Mixed Convection on Vertical Plate for Fluids of any Prandtl Number, *Wärme- und Stoffübertragung*, 22 (1988), 3, pp. 159-168

